Dyes and Pigments 103 (2014) 9–20

Contents lists available at ScienceDirect

Dyes and Pigments

journal homepage: www.elsevier.com/locate/dyepig

A facile ratiometric fluorescent chemodosimeter for hydrazine based on Ing–Manske hydrazinolysis and its applications in living cells

Mandapati V. Ramakrishnam Raju [a], Epperla Chandra Prakash [b], Huan-Cheng Chang [b], Hong-Cheu Lin [a,*]

[a] Department of Materials Science and Engineering, National Chiao Tung University, Hsinchu 300, Taiwan
[b] Institute of Atomic and Molecular Sciences, Academia Sinica, Taipei 106, Taiwan

ARTICLE INFO

Article history:
Received 17 September 2013
Received in revised form
11 November 2013
Accepted 12 November 2013
Available online 21 November 2013

Keywords:
Charge transfer
Fluorescent probe
Ing–Manske hydrazinolysis
pH effects
Semi-empirical calculations
Time resolved photoluminescence spectra

ABSTRACT

A facile and sensitive fluorescent probe for hydrazine was successfully constructed, displaying excellent colorimetric and ratiometric responses towards hydrazine via Ing–Manske hydrazinolysis conditions in semi-aqueous buffer solution. Semi-empirical calculations as well as spectroscopic results revealed the signalling mechanism of the current probe under hydrazinolysis conditions, in which hydrazine exclusively deprotected the phthalimide group by an intermediate of phthalhydrazide. Extensive screening of pH effects on the probe with the aid of proton nuclear magnetic resonance and mass spectrometry supported the distinctive and diverse ratiometric responses under hydrazinolysis and basic hydrolysis conditions. Time resolved photoluminescence measurements of the probe further confirmed its discernible ratiometric responses probed at respective wavelengths. A distinctive ratiometric response under basic hydrolysis conditions and a successful utilization of probe towards hydrazine detection in living cells are demonstrated.

1. Introduction

Developing efficient and reaction specific synthetic probes with better sensitivity for the detection of small molecule based analytes is of pivotal research interest owing to the toxic effects of many small molecules to humans and the environment [1]. Hydrazine is a strong reducing agent and highly reactive base [2]; moreover, its widespread usage is inevitable due to its vital roles in chemical, pharmaceutical, and agricultural industries involving catalysts, corrosion inhibitors, and pesticides [3]. Hydrazine is a well-known high-energy fuel in rocket propulsion and missile systems due to its improved detonable properties [4]. However, hydrazine is extremely toxic and easily absorbed by oral, dermal, and inhalation exposure routes. Previous studies on laboratory animals suggested that hydrazine is highly neurotoxic, mutagenic, and carcinogenic [5]. Thus, developing reliable and real-time fluorometric detection methods for the specific detection of hydrazine is warranted.

Conventionally, hydrazine was analysed by electrochemistry [6], chromatography-mass spectrometric [7], titrimetric [8] and gas chromatography [9] methods. However, those methods were often suffered in detecting hydrazine with low sensitivities. Despite their ease in detections with a trace amount of analytes by fluorometric methods possessing high sensitivity and selectivity functions; only a limited number of fluorescent small molecule based probes for hydrazine have been reported. Swager et al. developed the first fluorescent conjugated polymer for turn-on detection of trace amounts of hydrazine. [10] Chang et al. reported a selective detection of hydrazine by deprotection of a levulinate group [11]. Recently, Sessler and co-workers reported a trifluoroacetyl acetonate naphthalimide derivative that was formed a five membered heterocyclic compound, giving rise to a fluorescent turn-on response exclusively in the presence of hydrazine [12].

Developing ratiometric and reaction specific fluorescent chemodosimeters are often beneficial due to their specificity and built-in correction for quantitative measurement by the ratio of fluorescence intensities at two different wavelengths [13]. Chemodosimeters appended with specific protection groups for selective detections via target specific deprotection for various analytes have often been utilized effectively [14–16]. However, to date there are only two reported ratiometric probes based on hydrazine mediated ester deprotection [17] and hydrazone formation [18]. However, to the best of our knowledge a renowned NH_2 functional group

* Corresponding author. Tel.: +886 3 5712121x55305; fax: +886 3 5724727.
E-mail address: linhc@mail.nctu.edu.tw (H.-C. Lin).

0143-7208/$ – see front matter © 2013 Elsevier Ltd. All rights reserved.
http://dx.doi.org/10.1016/j.dyepig.2013.11.015

synthon phthalimide [19] has never been explored in the specific ratiometric detection of hydrazine. Excellent photophysical properties and outstanding intramolecular charge transfer (ICT) structures of hydrophilic 4-aminonaphthalimide make them expedient candidates in designing novel fluorescent probes [20]. However, facile ratiometric probes for hydrazine with selective and discriminative functions from other amine sources having potent biocompatibility within the biological pH range are required.

Herein, we developed a novel phthalimide protected 4-aminonaphthalimide for the specific and sensitive ratiometric detection of hydrazine via the Ing–Manske hydrazinolysis method [21], a key step in Gabriel amine synthesis [22] and thus, enabling ICT as well as living cell permeability. Probe **HZ** was synthesized by appending phthalimide group via CuI promoted aryl halide nucleophilic substitution of compound **2** with potassium phthalimide in high boiling dimethylacetamide (DMA) solvent in a moderate yield as depicted in Schemes 1 and 2.

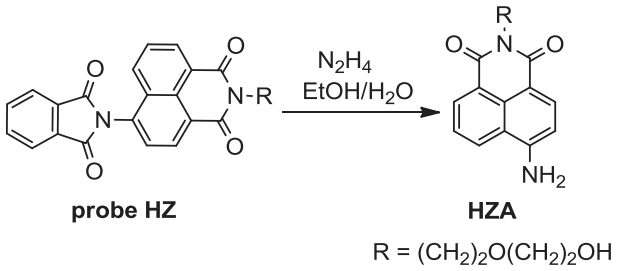

Scheme 1. Hydrazine mediated phthalimide deprotection of probe **HZ** to form **HZA**.

2. Experimental

2.1. General characterization methods

NMR spectra were recorded on Bruker Avance DRX300 Series (^{1}H: 300 MHz; ^{13}C: 75 MHz) at a constant temperature of 25 °C. Chemical shifts were reported in parts per million from low to high field and referenced to residual solvent ($CDCl_3$, d_6-DMSO: ^{1}H δ = 7.26, 2.49 ppm and ^{13}C δ = 77.23, 39.52 ppm, respectively). Coupling constant (J) were reported in hertz (Hz). UV–Vis spectra were recorded on the Jasco UV-600 spectrophotometer using 1 cm quartz cuvette. Fluorescence measurements were conducted with HITACHI 7000 Series Spectrophotometer. All emission and excitation spectra were corrected for the detector response and the lamp output. Melting points were determined using a Fargo MP-2D apparatus and are uncorrected. Elemental analyses were conducted on HERAEUS CHN-OS RAPID elemental analyser. Infrared spectroscopy data were collected using Perkin Elmer IR spectrophotometer. Solid sample were analysed using KBr pellet method. Time resolved photoluminescence (TRPL) spectra were measured using a home built single photon counting system with excitation from a 400 nm diode laser (Picoquant PDL-200, 50 ps fwhm, 2 MHz). The signals collected at the excitonic emissions of all sample solutions were connected to a time-correlated single photon counting card (TCSPC, Picoquant Timeharp 200). The emission decay data were analysed for **HZ**-hydrazine and **HZ**-hydroxide complex with biexponential kinetics, from which two decay components were derived; the lifetime values of (τ_1, τ_2) and pre-exponential factors (A_1, A_2) were determined. Confocal imaging was carried out using Leica TCS SP8 confocal fluorescence microscope, confocal fluorescence imaging with using 60× times oil objective. Semi-empirical PM3 calculations were calculated using Gaussian-09 suite [23].

2.2. Materials

All the reagents were purchased from commercial sources and used without further purification. All the solvents were HPLC grade; anhydrous solvents were obtained by passing through activated alumina column purification system, further dried by standard drying procedures. Solvents were degassed by freeze/thaw/pump cycle technique prior to use. 6-bromo-2-(2-(2-hydroxyethoxy)ethyl)-1*H*-benzo[de]isoquinoline-1,3(2*H*)-dione was prepared with a slight modification of previous literature [24].

2.3. Stock solutions

Standard solution of probe **HZ** (100 μM) were prepared in (1:9, v/v) in a mixture of water and ethanol solution. Prior to analysis the stock solution was diluted and pH of the solution was adjusted to about 7.2 using phosphate buffer saline (PBS) solution to deliver the final concentration of the probe (5 μM, pH = 7.2) in PBS-EtOH (1:9, v/v) solution. Hydrazine, other primary amines, metal ions, and anion stock solutions with concentration of (10 mM) were prepared, respectively in water. Before the titrations analytes were diluted to their desired volumes.

2.4. Cell culture and imaging

The human cervical cancer cell line (HeLa cells) were seeded onto cover slips at a concentration of (2×10^5 cells/mL) and cultured in Dulbecco's Modified Eagle's Medium (DMEM) and 10%

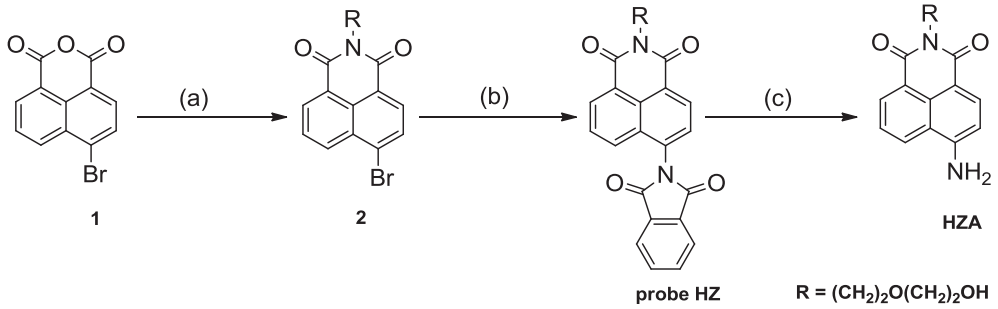

Scheme 2. Synthesis of Probe **HZ**. Reagents and Conditions: (a) 2-(2-aminoethoxy)ethanol, EtOH, reflux, 4 h, 88%; (b) potassium phthalimide, CuI, DMA, reflux, 1 day, 55%; (c) N_2H_4, EtOH/H_2O, 15 min, 70%.

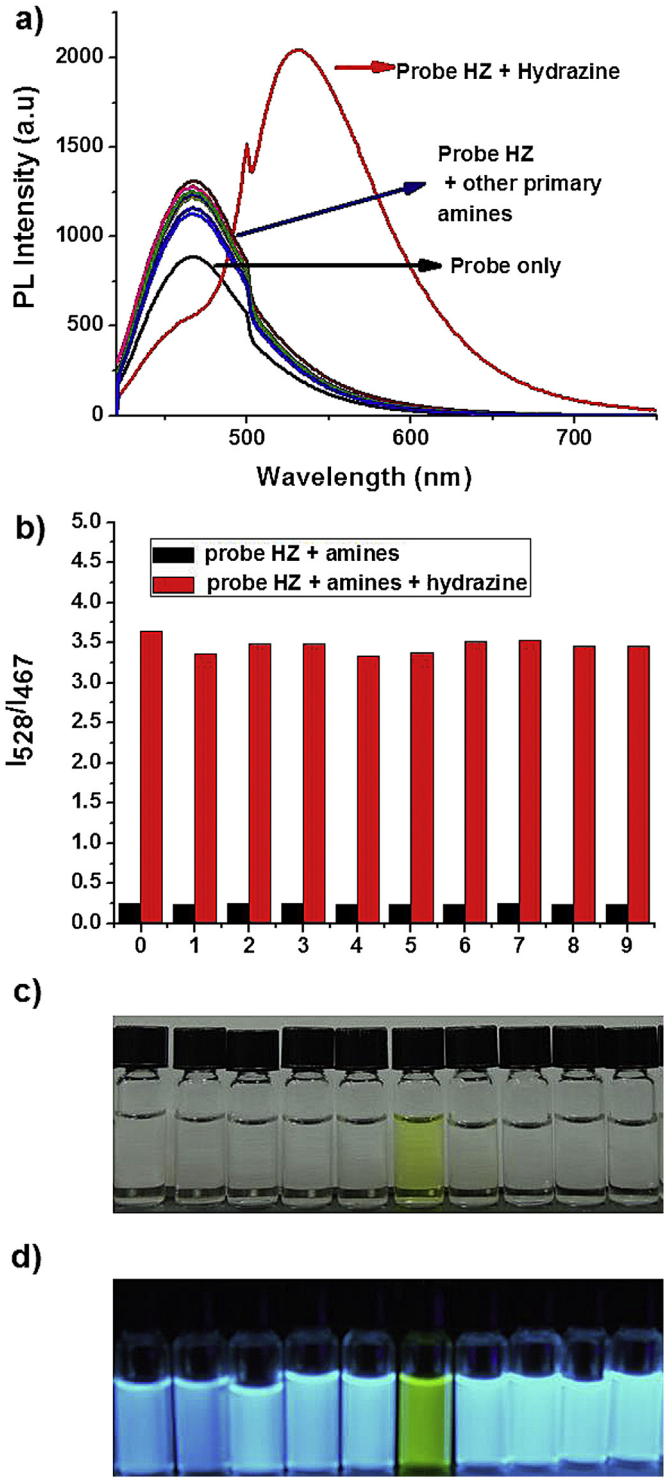

Fig. 1. (a) Fluorescence spectra of probe **HZ** in the presence of hydrazine and other representative primary amines. [**HZ**] = (5 μM), [hydrazine], and [primary amines] = (25 μM) in a mixture of PBS buffer solutions (pH 7.2, 10 mM) and EtOH (1:9, v/v); (b) Bars represent the fluorescence intensity ratio in the presence and absence of various amines. Black bar represent the addition of primary amines (25 μM) to probe **HZ** (5 μM). Red bars represent the subsequent addition of hydrazine (25 μM) to the solution. 0 = hydrazine, 1 = hydroxyl amine, 2 = urea, 3 = thiourea, 4 = monomethylamine, 5 = ethylenediamine, 6 = 1,4-diaminobutane, 7 = trans-1,2-diaminocyclohexane, 8 = aqueous ammonia, and 9 = guanidine nitrate, respectively. (c) and (d) UV–vis (naked eye) and fluorescence colour changes under (UV lamp 365 nm) of probe **HZ** (5 μM) with various amines (25 μM) sequentially from left to right hydroxyl amine, urea, thiourea, monomethylamine, ethylenediamine, hydrazine, 1,4-diaminobutane, trans-1,2-diaminocyclohexane, aqueous ammonia, and guanidine nitrate. λ_{ex} = 405 nm, Slits: 5 nm/5 nm. (For interpretation of the references to colour in this figure legend, the reader is referred to the web version of this article).

fetal bovine serum in an incubator (37 °C, 5% CO_2 and 25% O_2). After 30 h, the cover slips were rinsed slightly 3 times with PBS to remove the media and then cultured in PBS for later use. In view of imaging procedure, initially cells were incubated with 10 μM of probe **HZ** alone for 30 min at 37 °C and observed under microscope and then again the samples were treated with hydrazine (25 μM) and then incubated for 30 min and moved to the confocal stage. All the samples were slightly rinsed for 3 times with PBS buffer before observing them under the microscope. All the cell images were obtained with Leica TCS SP8 confocal fluorescence microscope using 60× times oil objective.

2.5. Synthesis of Probe *HZ*

2.5.1. Synthesis of 6-bromo-2-(2-(2-hydroxyethoxy)ethyl)-1H-benzo[de]isoquinoline-1,3(2H)-dione (*Compound 2*)

A mixture of 6-bromobenzo[de]isochromene-1,3-dione (**1**, 2.0 g, 7.22 mmol, 1.0 equiv) and 2-(2-aminoethoxy)ethanol (0.79 g, 7.58 mmol, 1.05 equiv) in ethanol (60 mL) was heated under reflux for 4 h, and slowly cooled down to room temperature. The solution further cooled overnight in a freezer and the precipitated compound was filtered and dried for overnight to get the compound **2** (2.31 g, 6.34 mol, 88%). Chemical formula: $C_{16}H_{14}BrNO_4$, Molecular weight: 364.19; m.p.140.9–142.4 °C.

IR (KBr, cm^{-1}): 3513, 3081, 2908, 2865, 1692,1588; **^{1}H NMR** (300 MHz, $CDCl_3$, 25 °C): δ (ppm) = 8.65 (d, J_d = 8.9 Hz, 1H), 8.55 (d, J_d = 8.9 Hz, 1H), 8.40 (d, J_d = 8.9 Hz, 1H), 8.03 (d, J_d = 8.9 Hz, 1H), 7.83 (t, J_t = 9.0 Hz, 1H), 4.43 (t, J_t = 6.1 Hz, 2H), 3.86 (t, J_t = 6.1 Hz, 2H), 3.68 (t, J_t = 6.0 Hz, 4H), 2.51 (br, 1H, OH); **^{13}C NMR** (75 MHz, $CDCl_3$, 298 K): δ (ppm) = 163.7, 133.2, 132.1, 131.3, 131.0, 130.4, 128.7, 128.0, 122.7, 121.9, 72.4, 68.3, 61.8, 39.7; **MS** (+**ESI-MS**): (*m*/*z*): Calcd for $C_{16}H_{14}BrNO_4$; 364.19; found: 364.0 $[M]^+$, 366.0 $[M + 2]^+$, 386 $[M + Na]^+$, $[M + Na+2]^+$; **Anal. Calcd**. for $C_{16}H_{14}BrNO_4$: C, 52.77; H, 3.87, N, 3.85 found; C, 52.68; H, 3.85, N, 3.86.

2.5.2. Synthesis of 6-(1,3-dioxoisoindolin-2-yl)-2-(2-(2-hydroxyethoxy)ethyl)-1H-benzo[de]isoquinoline-1,3(2H)-dione (Probe *HZ*)

A mixture of compound **2** (1.0 g, 2.74 mmol, 1.0 equiv), potassium phthalimide (0.53 g, 2.88 mmol, 1.05 equiv), and CuI (0.575 g, 3.00 mmol, 1.1 equiv) were taken in over dried 100 mL RBF, and the mixture was applied to 3 freeze–thaw–pump cycles. A freshly degassed DMA (60 mL) was added to the compound mixture and further degassed under argon atmosphere for 5 min, then reflux for 1 day. The solution was slowly cooled down to room temperature and poured into a beaker contains 200 g of crushed ice and stirred for 30 min, the resulted yellowish orange precipitate was filtered. The crude cake was dissolved in DCM (400 mL) and washed with brine solution (2 × 80 mL). The resulting solution was dried over $MgSO_4$ and evaporated under vacuum. The crude product was subjected to flash column chromatography (silica gel, Hexane/EA: 8/2 to 6/4) to yield a pure yellow coloured final probe **HZ** (0.65 g, 1.51 mmol, 55%). Chemical formula: $C_{24}H_{18}N_2O_6$, Molecular weight: 430.12; m.p. 256.8–258.2 °C.

IR (KBr, cm^{-1}): 3515, 3091, 2942, 2863, 1727, 1609, 1401, 1224, 1046; **^{1}H NMR** (300 MHz, $CDCl_3$, 25 °C): δ (ppm) = 8.72 (d, J_d = 8.9 Hz, 1H), 8.66 (d, J_d = 7.3 Hz, 1H), 8.05–8.00 (m, 3H), 7.91–7.88 (m, 2H), 7.79–7.73 (m, 2H), 4,47(t, J_t = 5.9 Hz, 2H), 3.86 (t,, J_t = 5.8 Hz, 2H), 3.67 (t, J_t = 3.9 Hz, 4H), 2.47 (br, 1H, OH); **^{13}C NMR** (75 MHz, $CDCl_3$, 298 K): δ (ppm) = 167.1, 164.2, 163.8, 135.1, 134.4, 132.1, 131.8, 131.2, 129.5, 129.3, 128.9, 127.9, 127.8, 124.4, 123.5, 123.2, 72.4, 68.4,

61.9, 39.8; **MS** (+**ESI-Ms**): (*m*/*z*): Calcd for $C_{24}H_{18}N_2O_6$; 430.12; found: 431.1 $[M + 1]^+$, 453.1 $[M + Na]^+$; **Anal. Calcd**. for $C_{24}H_{18}N_2O_6$: C, 66.97; H, 4.22 N, 6.51, found; C, 66.90; H, 4.20, N, 6.53.

*2.5.3. Synthesis of 6-amino-2-(2-(2-hydroxyethoxy)ethyl)-1H-benzo[de]isoquinoline-1,3(2H)-dione (**Compound HZA**)*

In an oven dried 25 mL RBF, probe **HZ** (0.050 g, 0.11 mmol, 1.0 equiv) was taken and dissolved in 8 mL of H_2O/EtOH (1/9, v/v) solution. Hydrazine (0.008 g, 0.24 mmol, 2.1 equiv, 0.5 M) solution was added in portion, an immediate colour change from deep yellow to pale yellow was observed. The reaction was continued for 15 min, at which time TLC showed complete deprotection of phthalimide. The resulted deep fluorescent solution was evaporated under vacuum, and then DCM (25 mL) was added to the crude product and stirred for 30 min, the resulted precipitate filtered through fine micron filter. The crude product was dissolved in minimum amount (4 mL) of MeOH and pentane (100 mL) was added and left under stirring for overnight. The resulted fine orange precipitate was filtered through fine micron filter and dried for overnight under vacuum to yield the final HZA product (0.024 g, 0.079 mmol, 70%). Chemical formula: $C_{16}H_{16}N_2O_4$, Molecular weight: 300.31; m.p. 204.6–206.0 °C.

IR (KBr, cm^{-1}): 3425, 3351, 3201, 2962, 2879, 1665, 1564, 1119; **^{1}H NMR** (300 MHz, d_6-DMSO, 25 °C): δ (ppm) = 8.60 (d, J_d = 8.9 Hz, 1H), 8.42 (d, J_d = 8.9 Hz, 1H), 8.18 (d, J_d = 8.9 Hz, 1H), 7.64 (t, J_t = 8.9 Hz, 1H), 7.45(s, 2H, NH_2), 6.83 (d, J_d = 8.1 Hz, 1H), 4.56 (s, 1H, OH), 4.19 (t, J_t = 6.0 Hz, 2H), 3.60 (t, J_t = 6.0 Hz, 2H), 3.44 (s, 4H); **^{13}C NMR** (75 MHz, d_6-DMSO $_3$, 298 K): δ (ppm) = 164.3, 163.3, 153.2, 134.5, 131.5, 130.2, 129.8, 124.4, 122.1, 119.8, 108.6, 107.8, 72.5, 67.5, 60.6, 38.8; **MS** (+**ESI-MS**): (*m*/*z*): Calcd for $C_{16}H_{16}N_2O_4$; 300.31; found: 301.3 $[M + 1]^+$, 323.1 $[M + Na]^+$; **Anal. Calcd**. for $C_{16}H_{16}N_2O_4$: C, 63.99; H, 5.37 N, 9.33, found; C, 63.89; H, 5.35, N, 9.31.

3. Results and discussion

*3.1. UV–Vis and fluorescence measurements of probe **HZ***

We primarily assessed the spectroscopic properties of the probe **HZ** in a mixture of phosphate buffer saline (PBS, pH = 7.2, 10 mM) and EtOH (1:9, v/v). The probe **HZ** (5 μM) without hydrazine exhibited a moderate UV–vis absorption band and a fluorescence emission band at 344 and 467 nm, respectively, owing to the electron withdrawing phthalimide protection group. However, upon the addition of hydrazine (20 μM, 4.0 equiv) we noticed an immediate colour change from colourless (344 nm) to yellow colour (439 nm) with a noticeable red-shift in the absorption band (Fig. S1). Concomitantly, a selective red-shift from 467 nm (blue) to 528 nm (yellowish green) was evidenced in the fluorescence emission spectra (see Fig. S2). The perceptible red-shifts in both UV–vis and fluorescence cases could be ascribed to the hydrazine promoted phthalimide deprotection with the release of electron donating amino grouped compound **HZA**. These observations indicated that the current probe **HZ** could be employed as a sensitive ratiometric sensor under physiological conditions.

We further examined fluorescence responses of the probe **HZ** over the various primary amine sources, such as hydroxylamine, urea, thiourea, monomethylamine, ethylenediamine, 1,4-diaminobutane, trans-1,2-diaminocyclohexane, ammonia, guanidine nitrate, and hydrazine to substantiate the selectivity of probe **HZ** (Fig. 1(b–d)). Upon the addition of 5 equiv of hydrazine, probe **HZ** (5 μM) illustrated a discernible ratiometric red-shift in Fig. 1(a). However, under similar conditions the other primary amine sources merely showed trivial responses in the emission behaviour.

To evaluate the quantitative analysis of probe **HZ**, we further measured the absorption and fluorescence changes of probe **HZ** (5 μM) by increasing the hydrazine concentrations from 0 to 20 μM. As shown in Fig. S3, upon the addition of hydrazine we noticed a gradual decline in the absorption band at 344 nm and a simultaneous increase of newly red-shifted absorption band at 439 nm. Likewise, the fluorescence emission band at 467 nm was gradually decreased with a concomitant upturn of a new red-shifted emission band at 528 nm (Fig. 2(a)), indicating a lucid colorimetric and ratiometric fluorescence response of probe **HZ**.

With the addition of hydrazine (20 μM), the emission intensity ratio at the two characteristic wavelengths of 467 and 528 nm increased to 15 fold (from 0.24 to 3.65). Importantly, the fluorescence response of probe **HZ** towards hydrazine showed a clear linear relationship (Fig. 2(b)) within the range of 0–7.5 μM, which allowed us to determine the detection limit of probe **HZ** for hydrazine (Fig. S4). Thus, the estimated detection limit was 4.2 nM (3σ/slope), which is comparable to those of previously reported ratiometric fluorescent sensors for hydrazine [18b,18c]. Moreover,

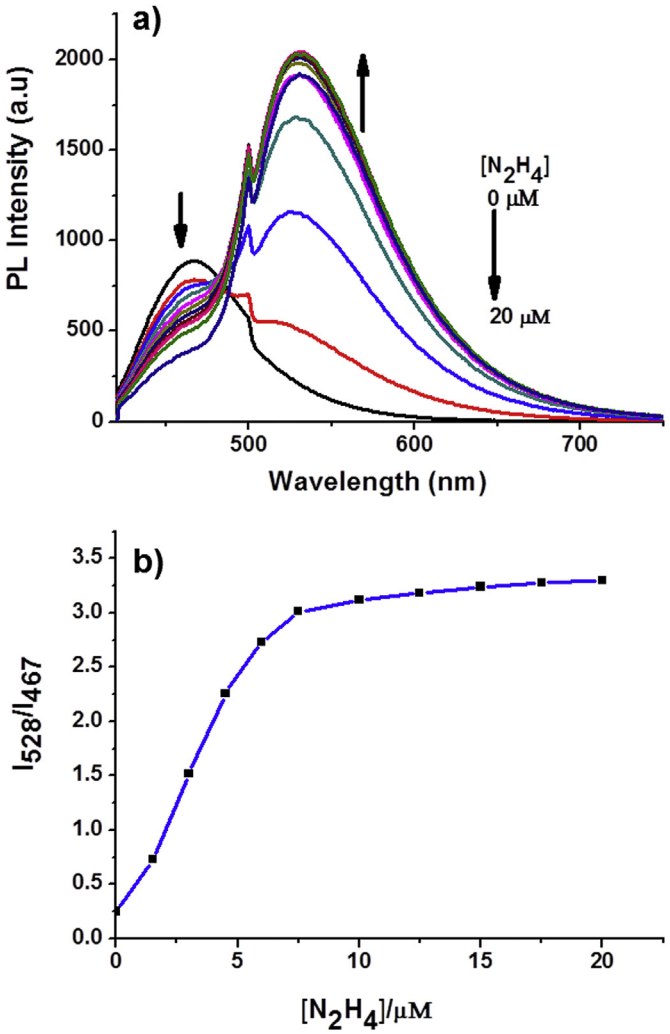

Fig. 2. (a) Fluorescence spectra of probe **HZ** (5 μM) upon the titration of hydrazine (0–20 μM) in a mixture of PBS buffer solutions (pH 7.2, 10 mM) in EtOH (1:9, v/v). Excitation λ = 405 nm, Slit: 5 nm/5 nm; (b) Ratiometric calibration curve $I_{528\ nm}/I_{467\ nm}$.

the probe showed no interferences of other competing analytes and satisfied the monitoring of threshold limit value (10 ppb) of hydrazine according to the U. S. Environmental Protection Agency (EPA) [25].

3.2. Theoretical and spectroscopic studies

To realize the ratiometric signalling mechanism of probe **HZ**, further strides were then made, in which the semi-empirical

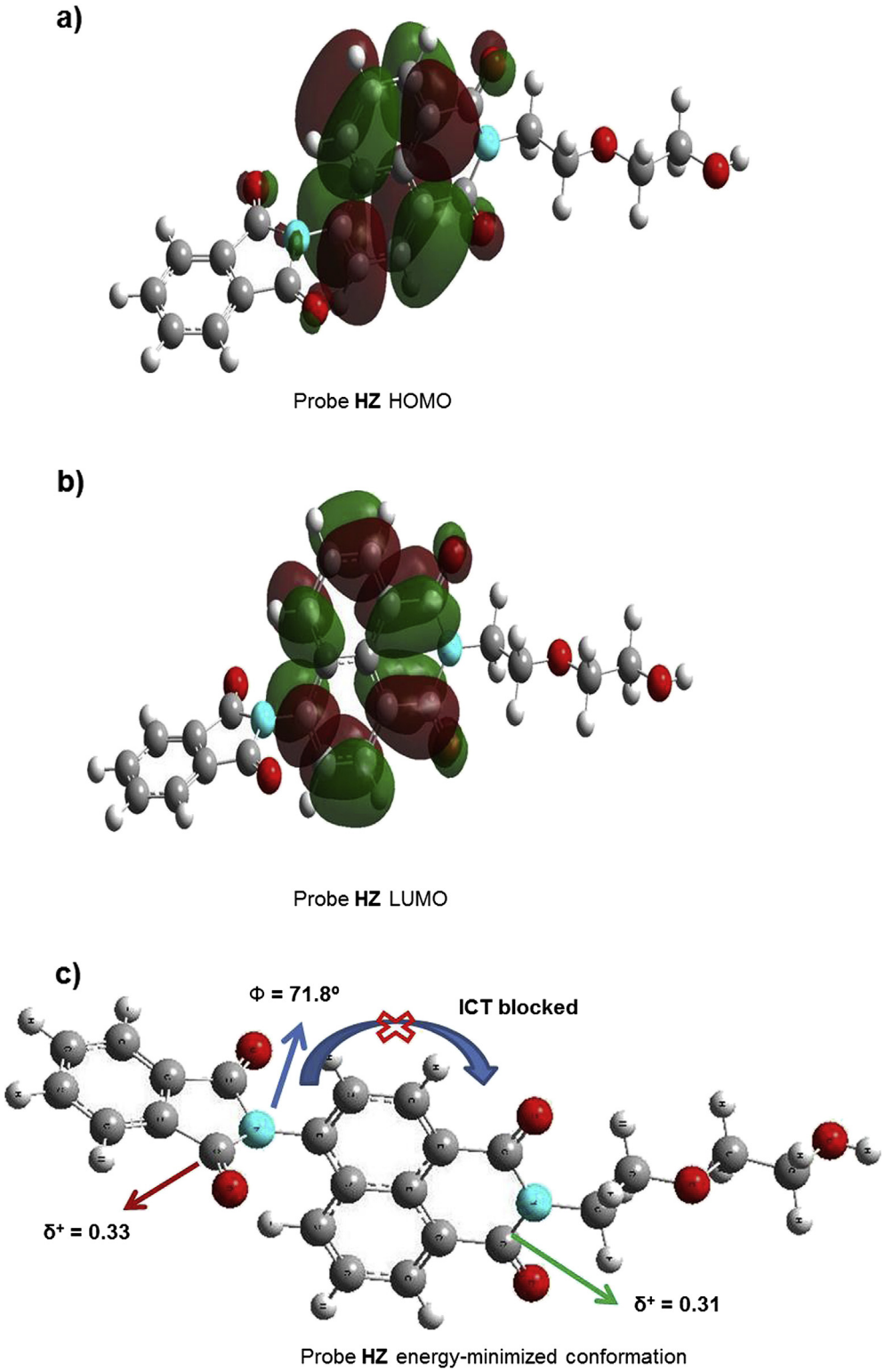

Fig. 3. (a) and (b) Semi-empirical PM3 optimized HOMO and LUMO frontier molecular orbital distributions of probe **HZ**, respectively; (c) energy-minimized geometry of probe **HZ**. Dihedral angle between phthalimide and naphthalimide plane was denoted in the picture, Mulliken charges of phthalimide and naphthalimide carbonyl carbons were depicted in picture (c) Colour coding of atoms blue = N, red = O, grey = C, and white = H, respectively. (For interpretation of the references to colour in this figure legend, the reader is referred to the web version of this article).

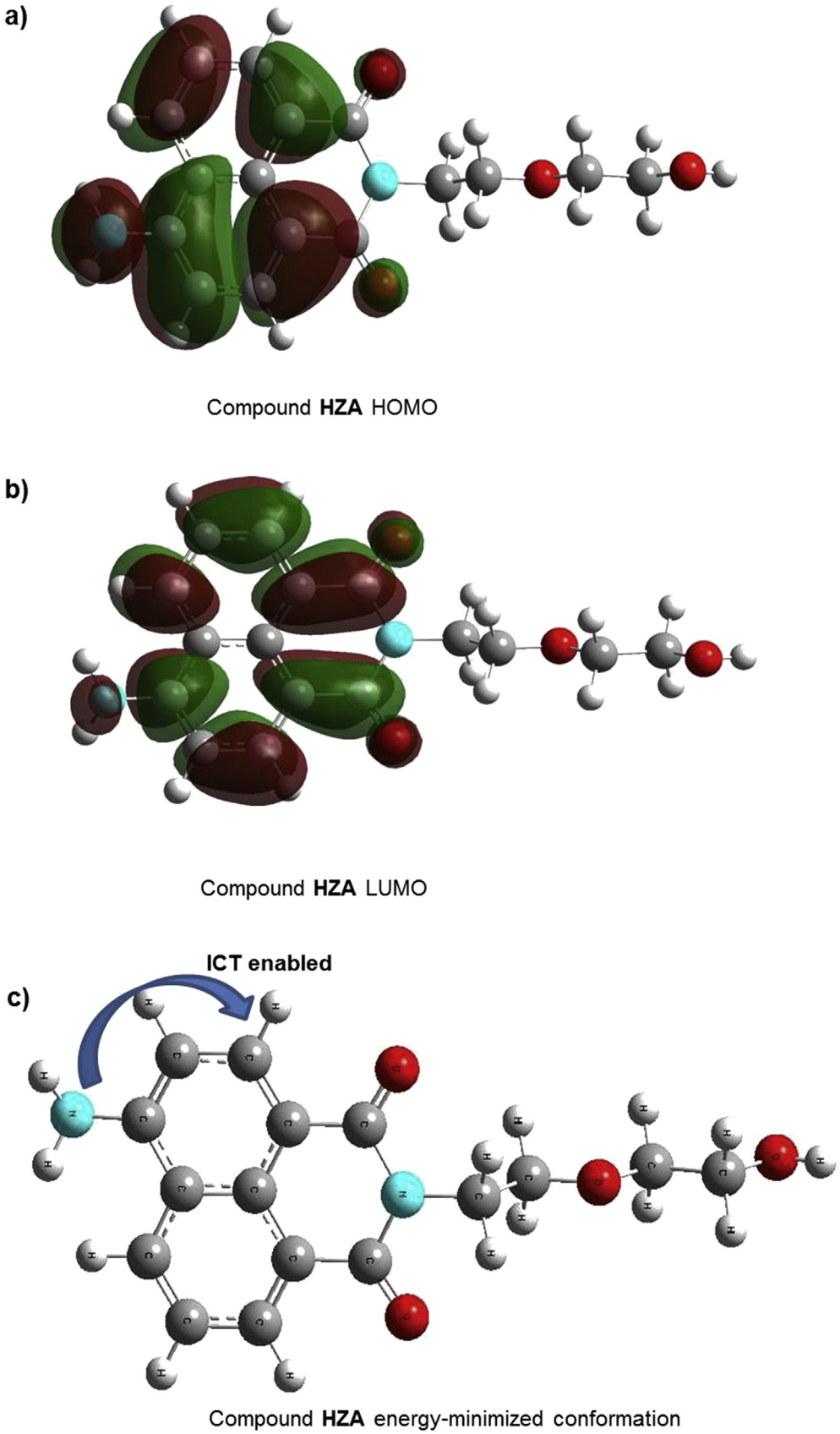

Fig. 4. (a) and (b) Semi-empirical PM3 optimized HOMO and LUMO frontier molecular orbital distributions of compound **HZA,** respectively; (c) energy-minimized geometry of compound **HZA**. Colour coding of atoms blue = N, red = O, grey = C, and white = H, respectively. (For interpretation of the references to colour in this figure legend, the reader is referred to the web version of this article).

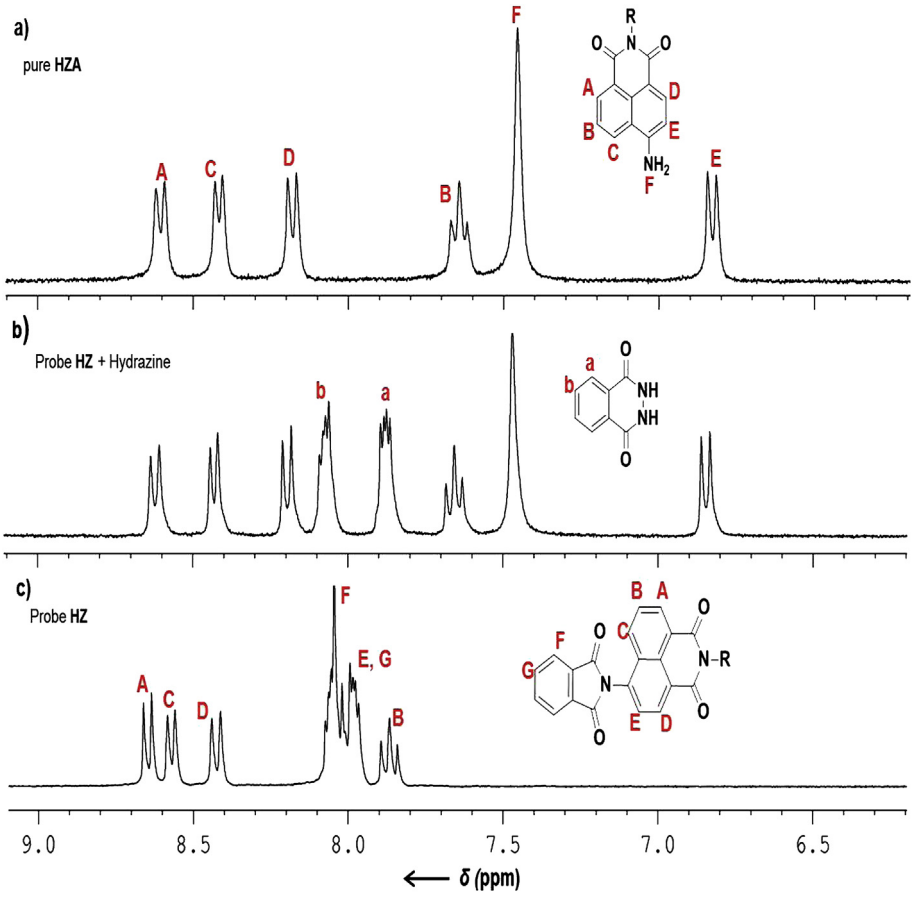

Fig. 5. ^{1}H NMR (d_6-DMSO, 300 MHz, 25 °C) stock plot. (a) pure **HZA** (3 mM), (b) probe **HZ** (3 mM) with the addition of hydrazine (2.0 equiv), and (c) probe **HZ** (3 mM).

theoretical calculations of probe **HZ** and compound **HZA** were studied. We observed that both HOMO and LUMO molecular orbital distributions in probe **HZ** were mainly resided on the naphthalimide moiety as shown in Fig. 3, which possessed a dihedral angle of $\Phi = 71.8^\circ$ with the distorted phthalimide unit. A further Mulliken charge analysis showed that the phthalimide carbonyl unit had a more electropositive character for carbon $\delta^+ = 0.33\ e$ in contrast to 0.31 e in the naphthalimide carbonyl unit.

The effective molecular orbital distribution across naphthalimide moiety indicated a weak ICT between phthalimide and naphthalimide. As we anticipated the hydrazinolysis of probe **HZ** changed the fate such that, with an enabling ICT from free donor amine group to naphthalimide moiety in the resulted compound

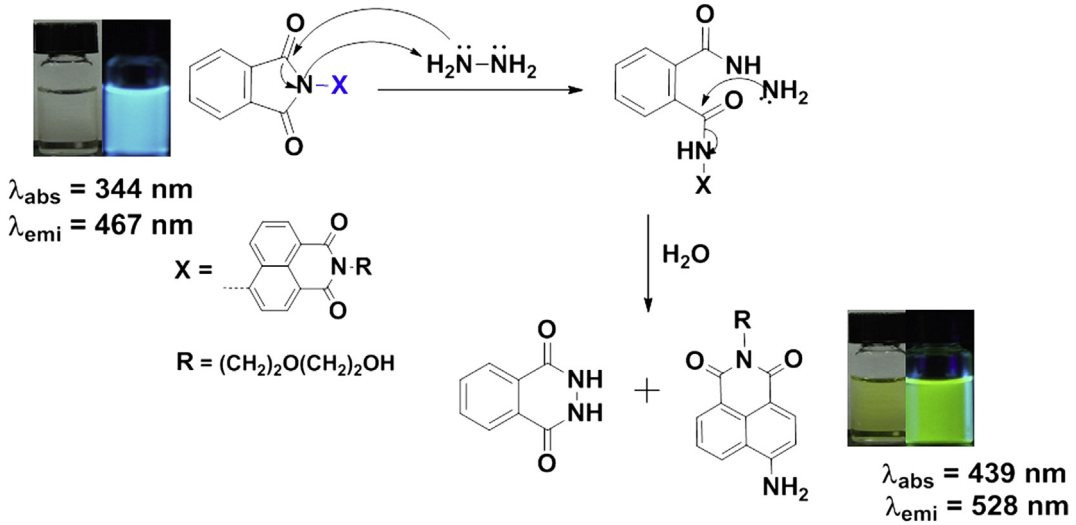

Scheme 3. The mechanism for hydrazine selective phthalimide deprotection of probe **HZ**.

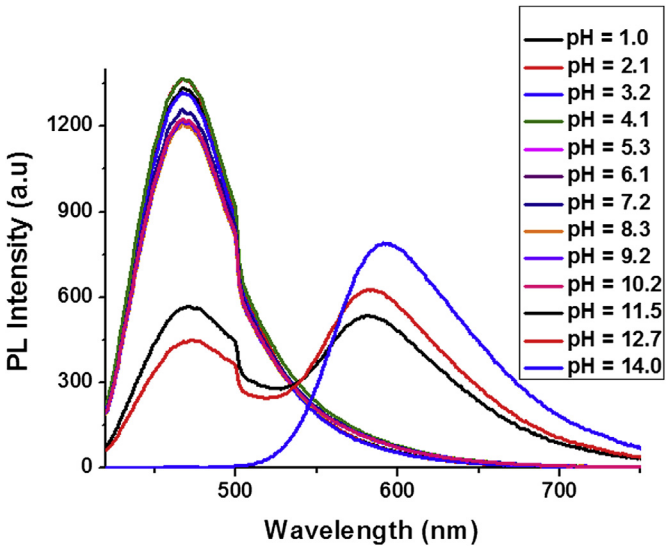

Fig. 6. Fluorescence intensity changes of probe **HZ** (6 μM) as a function of pH in a mixture of PBS buffer (pH 7.2, 10 mM) and EtOH (1:9), (v/v); λ_{ex} = 405 nm, Slits: 5 nm/5 nm.

HZA as depicted in Fig. 4. Moreover, ^{1}H NMR spectra of the free probe **HZ**, probe **HZ**-hydrazine complex, and isolated **HZA** in d_6-DMSO were compared in which the proton signals (a and b) corresponding to phthalhydrazide along with free amino grouped naphthalimide derivative appeared in the spectrum with the addition of hydrazine to probe (Fig. 5). Furthermore, ESI-MS analysis verified the release of phthalhydrazide during the hydrazine mediated phthalimide deprotection.

Based on these experimental and theoretical observations we outlined the plausible signalling mechanism. Deprotection of the phthalimide group of probe **HZ** proceeds first at the carbonyl position of phthalimide by the nucleophilic addition of hydrazine to leave the intermediate 2-(hydrazinecarbonyl)-*N*-naphthalimidobenzamide. [26] The subsequent nucleophile attacked on the carbonyl group to generate phthalhydrazide and 4-aminonaphthalimide, which possessed a unique colorimetric and ratiometric response (Scheme 3).

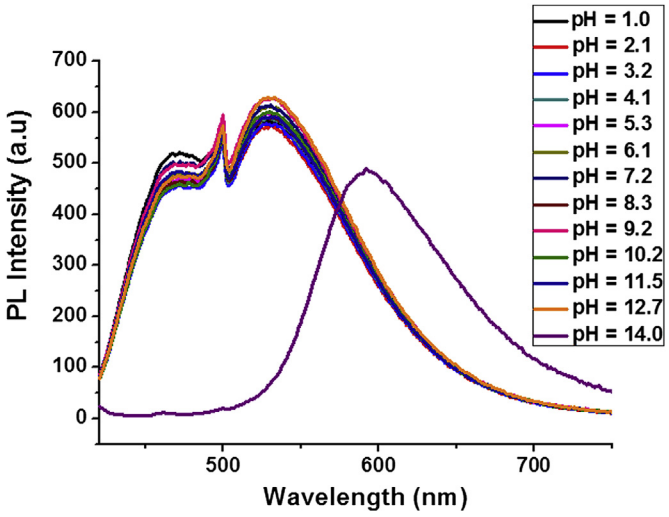

Fig. 7. Fluorescence intensity changes of probe **HZ** (6 μM) in the presence of hydrazine (12 μM) as a function of pH in a mixture of PBS buffer (pH 7.2, 10 mM) and EtOH (1:9), (v/v); λ_{ex} = 405 nm, Slits: 5 nm/5 nm.

3.3. Time effect on probe *HZ* ratiometric response

Considering the real-time detection of the probe **HZ** (6 μM) towards hydrazine, time-dependent fluoresce ratiometric changes of two characteristic wavelengths at 467 and 528 nm in the presence of hydrazine (30 μM) in a mixture buffer (PBS, pH 7.2, 10 mM) and EtOH (1:9, v/v) solutions (Fig. S5(a)) were verified. Delightfully, within 15 min the fluorescence ratiometric intensity ($I_{528\ nm}$/$I_{467\ nm}$) was increased to 5 fold with a perceivable dynamic nature (Fig. S5(b)). Obviously, the crossover point at 750 s for the two characteristic wavelengths 467 and 528 nm indicated the release of compound **HZA**, with enabling an effective ICT induced hydrazine selective ratiometric response of the probe **HZ**. Thus, the probe **HZ** could be useful for real-time detection of trace amounts of hydrazine.

3.4. Screening of probe selectivity over competing cations and anions

To fortify the selectivity of probe **HZ** to other common cations and anions (10 equiv), we investigated the fluorescence behaviour of probe **HZ**. However, the tested cations, such as Na^+, Ag^+, Ca^{2+}, Zn^{2+}, Cu^{2+}, Ni^{2+}, Cd^{2+}, Hg^{2+}, Pb^{2+}, Ag^{2+}, Fe^{3+} and Al^{3+}, on the probe **HZ** and probe **HZ**-hydrazine complex could not induce any noticeable changes as shown in Fig. S6. Similarly, we screened the effect of different anions, such as F^-, Cl^-, Br^-, I^-, AcO^-, NO_3^-, $H_2PO_4^-$, N_3^-, HCO_3^-, ClO_4^-, SO_4^{2-} and $S_2O_8^{2-}$, on probe **HZ** and probe **HZ**-hydrazine complex. As anticipated, none of these above anions could present distinct responses on probe **HZ** as well as probe **HZ**-hydrazine complex as depicted in Fig. S7. Based on these results it was inferred that probe **HZ** could be selectively and sensitively detect the hydrazine even in the presence of other competing cations and anions.

3.5. pH Effect on probe *HZ* and *HZ*-hydrazine complex

Since phthalimide was prone to basic hydrolysis and to further appreciate the probe **HZ** towards biological applications, we investigated the pH effects on fluorescence capabilities of **HZ** and **HZ**-hydrazine complex. The probe **HZ** possessed a stable response over the pH range of 1.0–10.0. Moreover, the **HZ**-hydrazine complex showed a stable ratiometric response within the biological pH range of 5.0–9.0 including acidic media as shown in Fig. 6 and Fig. 7. However, both the free probe **HZ** and **HZ**-hydrazine complex displayed a distinct ratiometric response (red colour) with a newly instigated fluorescence band at 596 nm in high basic pH range of 12–14 in contrast to the green fluorescence of probe-**HZ**-hydrazine within the pH range of 1–10. This photophysical study gave a clue that the ratiometric response of probe **HZ** under basic hydrolysis condition was quite different in comparison with probe **HZ** hydrazinolysis.

Further spectroscopic (^{1}H NMR & ESI-MS) analyses were conducted to obtain further insight into the distinctive ratiometric response of probe **HZ** in high basic solution. We noticed a different chemical shift pattern for probe **HZ** in the presence of high basic solution in contrast to hydrazinolysis as shown in Fig. 8. A readily observed colour change from colourless to red as well bright red fluorescence compared with initial blue fluorescence was observed immediately after hydroxide addition in the NMR tube. ESI-MS analysis of probe **HZ** in both positive and negative modes were verified to know the plausible reaction fragments in acidic, basic, and hydrazinolysis conditions, as shown in Figs. S8–S10. Regardless of phthalimide itself in acidic nature, the probe could not present any observable changes in acidic media as we noticed in photophysical titrations. However, we observed distinct mass fragments

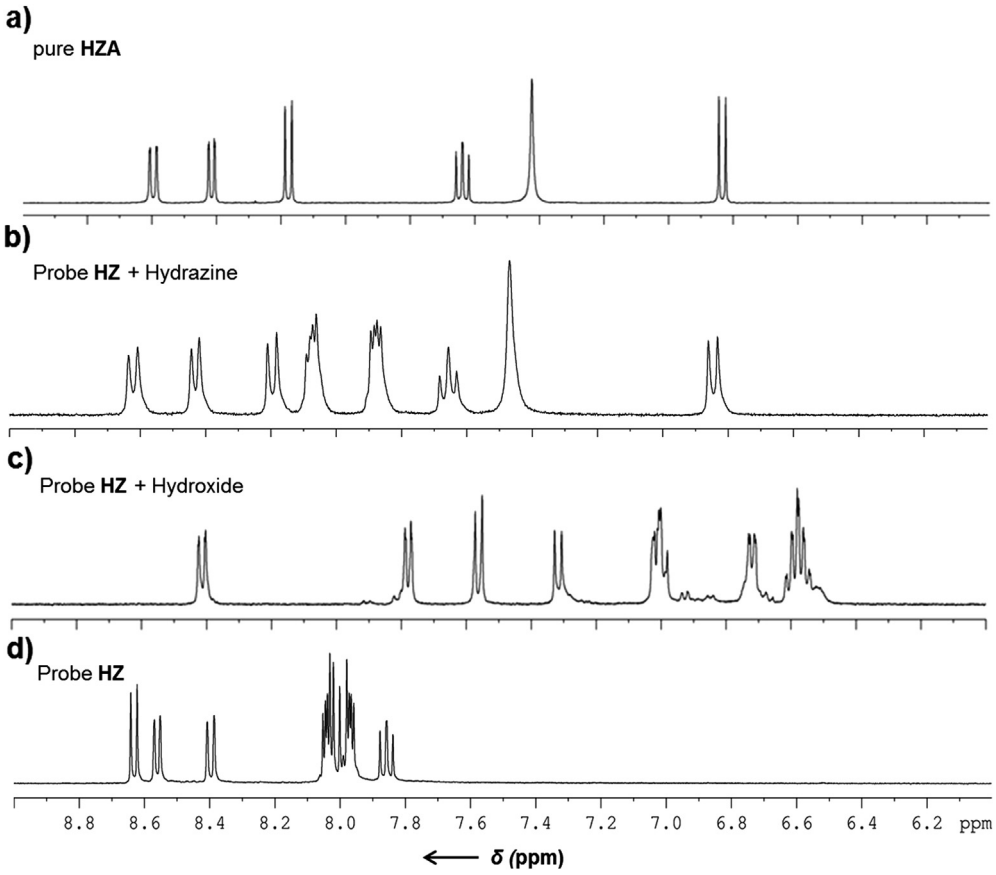

Fig. 8. ^{1}H NMR (d_6-DMSO, 400 MHz, 25 °C) stock plot. (a) pure **HZA** (3 mM); (b) probe **HZ** (3 mM) with the addition of hydrazine (2.0 equiv); (c) probe **HZ** with the addition of hydroxide (2.0 equiv) in D_2O; (d) probe **HZ** (3 mM).

in basic hydrolysis which was consistent with above photophysical and spectroscopic studies.

Based on this evidence we draw out the plausible intermediates in acidic, hydrazinolysis and basic conditions for probe **HZ** as depicted in Scheme 4. These results clearly suggested that the current probe could be employed in living cells with better cell permeability without interference from the pH effects within the biological pH range and acidic media. Although the probe has a pure aqueous solubility, it gave long-time and trivial responses towards hydrazine and other primary amines owing to the reduced nucleophilicity of amines by the strong water-amine H-bonding in aqueous solutions in contrast to ethanol buffer solutions.

3.6. Time resolved photoluminescence measurements

To corroborate the above photophysical studies, time resolved photoluminescence measurements (excited at 405 nm) were conducted for the free probe **HZ**, **HZ**-hydrazine complex, and **HZ**-hydroxide complex by probing at 467, 528, and 596 nm, respectively. Probe **HZ** showed a monoexponential fluorescence decay with the lifetime of (τ_1) 4.31 ns, but we observed a biexponential fluorescence decay with the life time values of $\tau_1 = 7.91$ ns (87.4%) and $\tau_2 = 1.86$ ns (12.6%) for **HZ**-hydrazine complex as shown in Fig. 9. Lifetime component τ_2 with the shorter value could be ascribed to the hydrazine mediated phthalimide deprotection with the release of electron donating amino group in compound **HZA**, and the lifetime component τ_1 represents intrinsic fluorescence of naphthalimide fluorophore. Significantly, we noticed a distinctive lifetime pattern for **HZ**-hydroxide complex as shown in Fig. S11. Time resolved fluorescence became biexponential decay with the life time values of $\tau_1 = 18.38$ ns (2.15%) and $\tau_2 = 2.63$ ns (97.85%). The larger variation of the lifetime components indicated a unique ratiometric response under the basic hydrolysis of probe **HZ**. Moreover, these drastic lifetime changes in contrast to **HZ**-hydrazine could be attributed to the newly instigated red fluorescence peak at 596 nm. Based on the lifetime measurements, we can infer that probe **HZ** showed diverse and characteristic ratiometric responses under hydrazinolysis and basic hydrolysis depending on the nucleophilicity of analytes. We were able to show the facile and differentiable ratiometric chemodosimeteric approach for the detection of hydrazine even in the presence of competing basic media.

3.7. Confocal imaging

Encouraged by the foregoing performance of probe **HZ**, we next sought to apply probe **HZ** for fluorescence ratiometric imaging of hydrazine in living cells. Hydrazine could be detected in the human cervical cancer cell line (HeLa cells). The Cells incubated with probe **HZ** (10 μM) alone for 30 min at 37 °C showed blue fluorescence (Fig. 10(a) and (b)). However, a perceptible green fluorescence was monitored in the cells after treatment with hydrazine (25 μM) see Fig. 10(c) and (d). Apparent changes denoted that probe **HZ** was cell membrane permeable and capable of ratiometric imaging of hydrazine in the living cells.

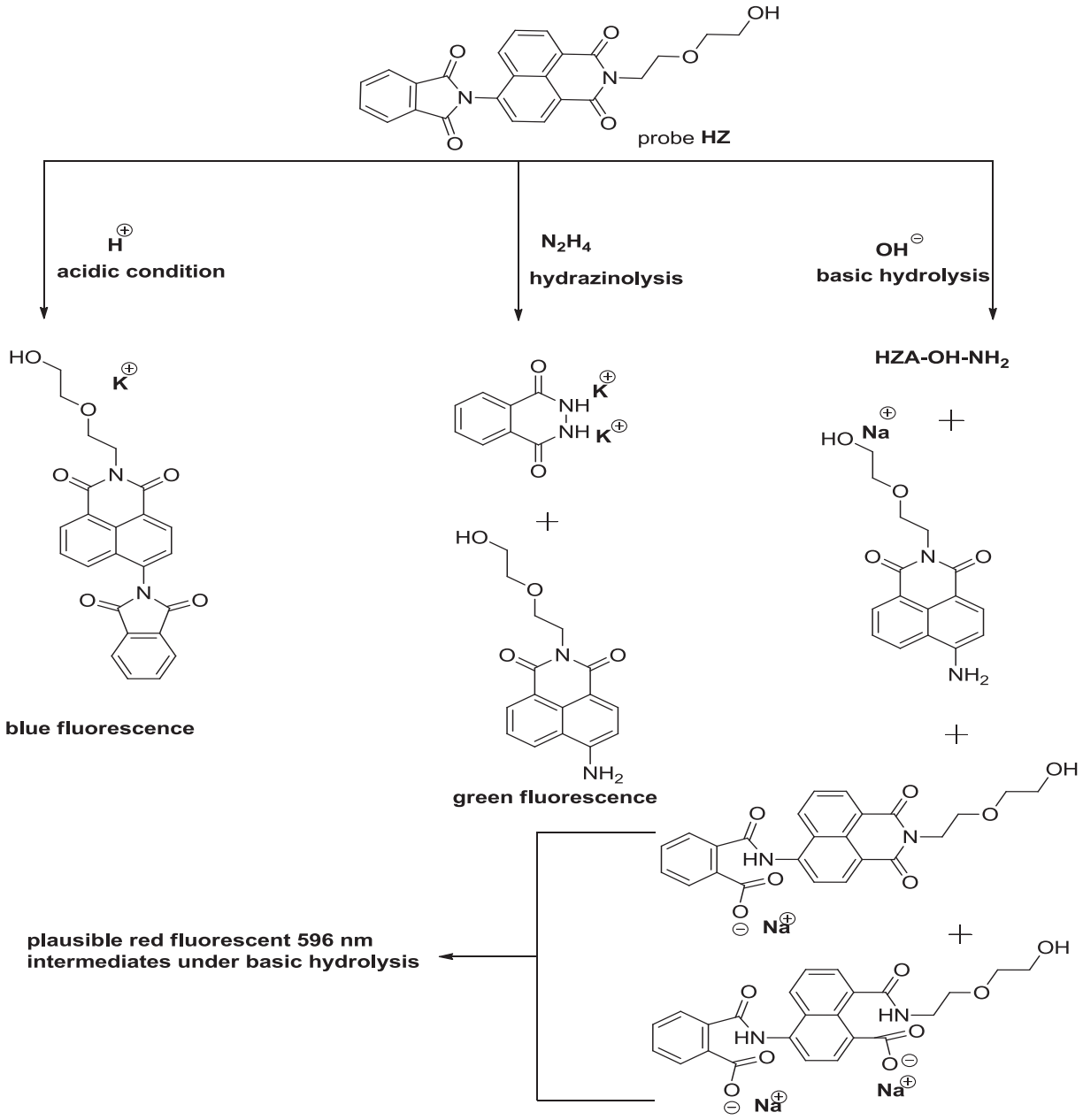

Scheme 4. Plausible reaction intermediates of probe **HZ** under acidic, basic hydrolysis and hydrazinolysis conditions.

4. Conclusions

In summary, we have developed a facile and sensitive fluorescent probe for hydrazine based on Ing–Manske hydrazinolysis method under mild conditions. The probe **HZ** showed a selective colorimetric and fluorescent ratiometric response towards hydrazine in the semi-aqueous buffer solution with a low detection limit. The unique ratiometric response under basic hydrolysis further differentiated from probe **HZ** hydrazinolysis. Current probe showed a stable ratiometric response including acidic and biological pH ranges. Theoretical and time resolved photoluminescence measurements further confirmed the distinctive ratiometric modes of probe **HZ** under hydrazinolysis and basic hydrolysis conditions. Hence, the hydrazinolysis-based ratiometric fluorescent probe was developed for the first time in this report. Pivotal confocal imaging of hydrazine in living cells also demonstrated that probe **HZ** could be favourable for biological applications.

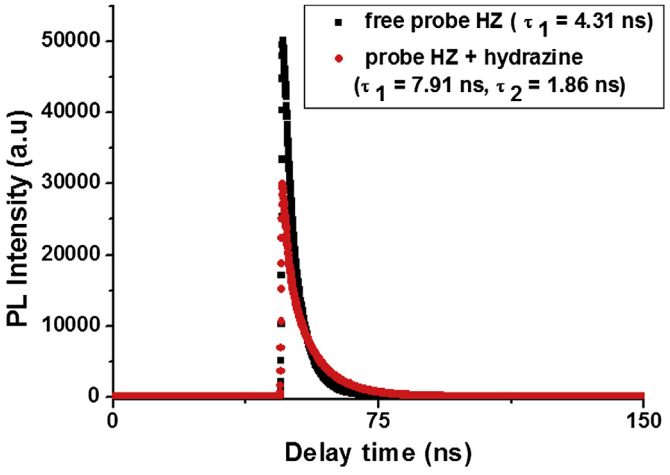

Fig. 9. Time resolved fluorescence spectral changes of probe **HZ** and **HZ**-hydrazine complex.

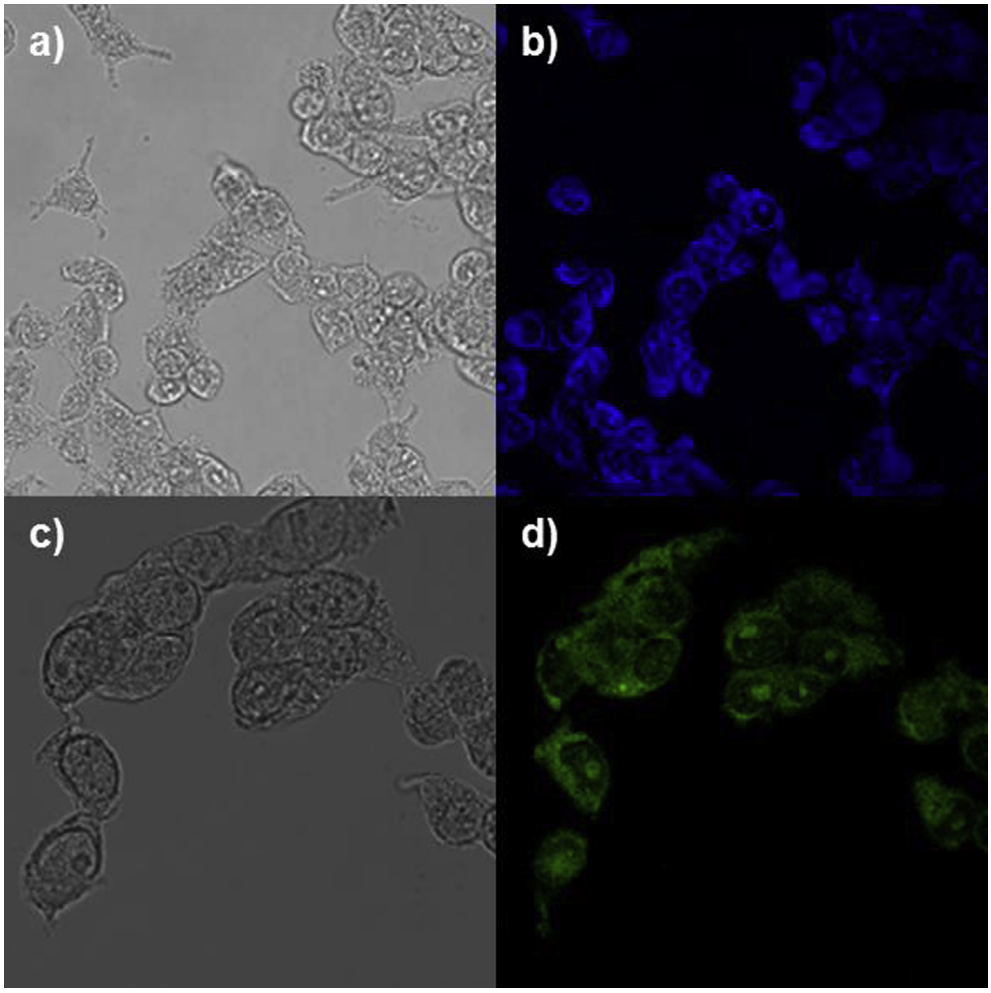

Fig. 10. Confocal microscopic images of HeLa cells incubated with 10 μM probe **HZ** for 30 min (b) and then further incubated with 25 μM hydrazine for 30 min (d); (a), (c) Bright-field transmission image of HeLa cells in (b) and (d), respectively. $\lambda_{ex} = 405$ nm.

Acknowledgements

We thank the National Science Council of Taiwan (ROC) for financial supports of this project through NSC 101-2113-M-009-013-MY2 and NSC 99-2221-E-009-008-MY2.

Appendix A. Supplementary data

Supplementary data related to this article can be found at http://dx.doi.org/10.1016/j.dyepig.2013.11.015

References

[1] (a) Rettig W, Strehmel B, Schrader S, Seifert H. Applied fluorescence in chemistry, biology and medicine. New York: Springer; 1999;
(b) Buffle J, Horvai G. In situ monitoring of aquatic systems; chemical analysis and speciation. New York: Wiley; 2001;
(c) Diamond D, Coyle S, Scarmagnani S, Hayes J. Wireless sensor networks and chemo-/biosensing. Chem Rev 2008;108:652–79;
(d) Shapira A, Livney YD, Broxterman HJ, Assaraf YG. Nanomedicine for targeted cancer therapy: towards the overcoming of drug resistance. Drug Resist Updat 2011;14:150–63.

[2] (a) Schiessl HW. Kirk-Othmer encyclopedia of chemical technology. John Wiley & Sons, Inc.; 2000. p. 562;
(b) Garrod S, Bollard ME, Nicholls AW, Connor SC, Connelly J, Nicholson JK, et al. Integrated metabonomic analysis of the multiorgan effects of hydrazine toxicity in the rat. Chem Res Toxicol 2005;18:115–22.

[3] (a) Narayanan SS, Scholz F. A comparative study of the electrocatalytic activities of some metal hexacyanoferrates for the oxidation of hydrazine. Electroanalysis 1999;11:465–9;
(b) Ragnarsson U. Synthetic methodology for alkyl substituted hydrazines. Chem Soc Rev 2001;30:205–13.

[4] (a) Hannum JAE. Recent developments in the technology of propellant hydrazines. Chemical Propulsion Information Agency; June 1982. CPTR 82–15;
(b) Schmidt EW. Hydrazine and its derivatives: preparation, properties, applications. New York: Wiley; 1984;
(c) Wang J. Hydrazine detection using a tyrosinase-based inhibition biosensor. Anal Chem 1995;67:3824–7;
(d) Zelnick SD, Mattie DR, Stepaniak PC. Occupational exposure to hydrazines: treatment of acute central nervous system toxicity. Aviat Space Environ Med 2003;74:1285–91;
(e) Serov A, Kwak C. Direct hydrazine fuel cells: a review. Appl Catal B 2010;98:1–9.

[5] (a) Vernot EH, MacEwen JD, Bruner RH, Haus CC, Kinkead ER. Long-term inhalation toxicity of hydrazine. Fundam Appl Toxicol 1985;5:1050–64;
(b) Lyon. International agency for research on cancer: re-evaluation of some organic chemicals, hydrazine, and hydrogen peroxideIn IARC monographs on the evaluation of carcinogenic risk of chemicals to humans, vol. 71. IARC; 1999. pp. 991–1013;
(c) Golabi SM, Zare HR. Electrocatalytic oxidation of hydrazine at a chlorogenic acid (CGA) modified glassy carbon electrode. J Electroanal Chem 1999;465:168–76.

[6] (a) Hou W, Wang E. Flow-injection amperometric detection of hydrazine by electrocatalytic oxidation at a prussian blue-film modified electrode. Anal Chim Acta 1992;257:275–80;
(b) Xia H, Li HL. Electrooxidation of hydrazine catalysed by 4-hydroxy-2,2,6,6-tetramethyl-piperidininyloxy (TEMPOL). J Electroanal Chem 1997;430:183–7;
(c) Casella IG, Guascito MR, Salvi AM, Desimoni E. Catalytic oxidation and flow detection of hydrazine compounds at a nifion/ruthenium(III) chemically modified electrode. Anal Chim Acta 1997;354:333–41;
(d) Guerra SV, Xavier CR, Nakagaki S, Kubota LT. Electrochemical behavior of copper porphyrin synthesized into zeolite cavity: a sensor for hydrazine.

Electroanlaysis 1998;10:462–6;
(e) Li X, Zhang S, Sun C. Fabrication of covalently attached multilayer film electrode containing cobalt phthalocyanine and its electrocalalytic oxidation of hydrazine. J Electroanal Chem 2003;553:139–45;
(f) Revenga-Parra M, Lorenzo E, Pariente F. Synthesis and electrocalalytic activity towards oxidation of hydrazine a new family of hydroquinone salophen derivaives: application to the construction of hydrazine sensors. Sens Actuators B Chem 2005;107:678–87;
(g) Batchelor-McAuley B, Banks CE, Simm AO, Jones TGJ, Compton RG. The electroanalytical detection of hydrazine: a comparision of the use of palladium nanoparticles supported on boron-doped diamond and palladium plated BDD microdisc array. Analyst 2006;131:106–10.

[7] Oh JA, Park JH, Shin HS. Sensitive determination of hydrazine in water by gas chromatography-mass spectrometry after derivatization of with *ortho*-phthalaldehyde. Anal Chim Acta 2013;769:79–83.

[8] He ZK, Fuhrmann B, Spohn U. Coulometric microflow titrations with chemiluminescent and amperometric equivalence point detection: bromimetric titration of low concentration of hydrazine and ammonium. Anal Chim Acta 2000;409:83–91.

[9] Liu YY, Schmeltz I, Hoffmann D. Chemical studies on tobacco smoke: quantitative analysis of hydrazine in tobacco and cigarette smoke. Anal Chem 1974;46:885–9.

[10] Thomas SW, Swager TM. Trace hydrazine detection with fluorescent conjugated polymers: a turn-on sensory mechanism. Adv Mater 2006;18:1047–50.

[11] Choi MG, Hwang J, Moon JO, Sung J, Chang SK. Hydrazine-selective chromogenic and fluorogenic probe based on levulinated coumarin. Org Lett 2011;13:5260–3.

[12] Lee MH, Yoon B, Kim JS, Sessler JL. Naphthalimide trifluoroacetyl acetonate: a hydrazine- selective chemodosimeteric sensor. Chem Sci 2013;4:4121–6. http://dx.doi.org/10.1039/c3sc51813b.

[13] (a) Chen X, Tian X, Shin I, Yoon J. Fluorescent and luminescent probes for detection of reactive oxygen and nitrogen species. Chem Soc Rev 2011;40:4783–804;
(b) Chang JF, Zhou Y, Yoon J, Kim JS. Recent progress in fluorescent and colorimetric for detection of precious metal ions (silver, gold and platinum ions). Chem Soc Rev 2011;40:3416–29;
(c) Park S, Kim W, Swamy KMK, Lee HY, Jung JY, Kim G, et al. Rhodamine hydrazone derivatives bearing thiophene group as fluorescent chemosensors for Hg^{2+}. Dyes Pigment 2013;99:323–8.

[14] (a) Jiang J, Liu W, Cheng J, Yang L, Jiang H, Bai D, et al. A sensitive colorimetric and ratiometric fluorescent probe for mercury species in aqueous solution and living cells. Chem Commun 2012;48:8371–3;
(b) Das P, Mandal AK, Chandar NB, Baidya M, Bhatt HB, Ganguly B, et al. New chemodosimeteric reagents as ratiometric probes for cysteine and homocysteine and possible detection in living cells and in blood plasma. Chem Eur J 2012;18:15382–93;
(c) Wang L, Zhou Q, Zhu B, Yan L, Ma Z, Du B, et al. A colorimetric and fluorescent chemodosimeter for discriminative and simultaneous quantification of cysteine and homocysteine. Dyes Pigment 2012;95:275–9.(d) Hu ZQ, Zhuang WM, Li M, Liu MD, Wen LR, Li CX. Highly sensitive and selective fluorescent chemodosimeter for Hg^{2+} based on thiorhodamine 6G–amide and its application for biological imaging. Dyes Pigment 2013;98:286–9;
(e) Huang L, Liu Y, Ma C, Xi P, Kou W, Zeng Z. A fluorescent probe for the determination of Ce^{4+} in aqueous media. Dyes Pigment 2013;96:770–3.

[15] Du J, Hu M, Fan J, Peng X. Fluorescent chemodosimeters using "mild" chemical events for the detection of small anions and cations in biological and environment media. Chem Soc Rev 2012;41:4511–35.

[16] (a) Maity D, Govindaraju T. A differentially selective sensor with fluorescence turn-on response to Zn^{2+} and dual mode ratiometric response to Al^{3+} in aqueous media. Chem Commun 2012;48:1039–41;
(b) Choi MG, Moon JK, Bae J, Lee W, Chang SK. Dual signalling of hydrazine by selective deprotection of chlorofluorescein and resorufin acetates. Org Biomol Chem 2013;11:2961–5;
(c) Xu Y, Li B, Li W, Zhao J, Sun S, Pang Y. "ICT-not-quenching" near infrared ratiometric fluorescent detection of picric acid in aqueous media. Chem Commun 2013;49:4764–6.

[17] Li K, Xu HR, Yu KK, Hou JT, Yu XQ. A coumarin based chromogenic and ratiometric probe for hydrazine. Anal Methods 2013;5:2653–6.

[18] (a) Chen X, Xiang Y, Li Z, Tong A. Sensitive and selective fluorescence determination of trace hydrazine in aqueous solution utilizing 5-chlorosalcicylalehyde. Anal Chim Acta 2008;625:41–6;
(b) Fan J, Sun W, Hu M, Cao J, Cheng G, Dong H, et al. An ICT-based ratiometric probe for hydrazine and its application in live cells. Chem Commun 2012;48:8117–9;
(c) Hu C, Sun W, Cao J, Gao P, Fan J, Song F, et al. A ratiometric near-infrared fluorescent probe for hydrazine and its *in vivo* applications. Org Lett 2013;15:4022–5.

[19] Khan MN. Kinetic evidence for the occurrence of a stepwise mechanism in hydrozinolysis of phthalimide. J Org Chem 1995;60:4536–41.

[20] (a) Duke MR, Veale EB, Kruger PE, Gunnlaugsson T. Colorimetric and fluorescent anion sensors: an overview of in the recent developments in the use of 1,8-naphthalimide-based chemosensors. Chem Soc Rev 2010;39:3936–53;
(b) Georgiev NI, Bojinov VB, Nikolov PS. The design, synthesis and photophysical properties of two novel 1,8-naphthalimide fluorescent pH sensors based on PET and ICT. Dyes Pigment 2011;88:350–7;
(c) Wang M, Xu Z, Wang X, Cui J. A fluorescent and colorimetric chemosensor for nitric oxide based on 1,8-naphthalimide. Dyes Pigment 2013;96:333–7.

[21] March J. Advanced organic chemistry: reactions, mechanisms and structures. 2nd ed. Tokyo: McGraw-Hill Kogakusha, Ltd.; 1977. p. 388.

[22] (a) Bolhoter WA, Sheehan JC. An improved procedure for the condensation of potassium phthalimide with organic halides. J Am Chem Soc 1950;72:2786–8;
(b) Gibson MS, Bradshaw RW. The Gabriel synthesis of primary amines. Angew Chem Int Ed 1968;7:919–30.

[23] Frisch MJ et al. Gaussian, Inc.: Wallingford CT; 2009.

[24] Tian H, Gan J, Chen K, He J, Song QL, Hou XY. Positive and negative fluorescent imaging induced by naphthalimide polymers. J Mater Chem 2002;12:1262–7.

[25] (a) Shortreed M, Kopelman R, Kuhn M, Hoyland B. Fluorescent fiber-optic calcium sensor for physiological measurements. Anal Chem 1996;68:1414–8;
(b) Umar A, Rahman MM, Kim SH, Hahn YB. Zinc oxide nanonail based chemical sensor for hydrazine detection. Chem Commun 2008:166–8.

[26] (a) Ing HR, Manske RHF. A modification of the Gabriel synthesis of amines. J Chem Soc 1926:2348–51;
(b) Ariffin A, Khan MN, Lan LC, May FY, Yun CS. Suggested improved method for the Ing–Manske and related reactions for the second step of Gabriel synthesis of primary amines. Synth Commun 2004;34:4439–45.